Phase problem and the Radon transform

Andrei V. Bronnikov

Bronnikov Algorithms
The Netherlands

- The Radon transform and applications
- Inverse problem of phase-contrast CT
- Fundamental theorem
- Image reconstruction algorithms
- Phantom studies
- Experimental data

The Radon transform (J. Radon, 1917)

$$\hat{f}_{\theta,s} = \int_{Line\ (\theta,s)} f\, dl$$

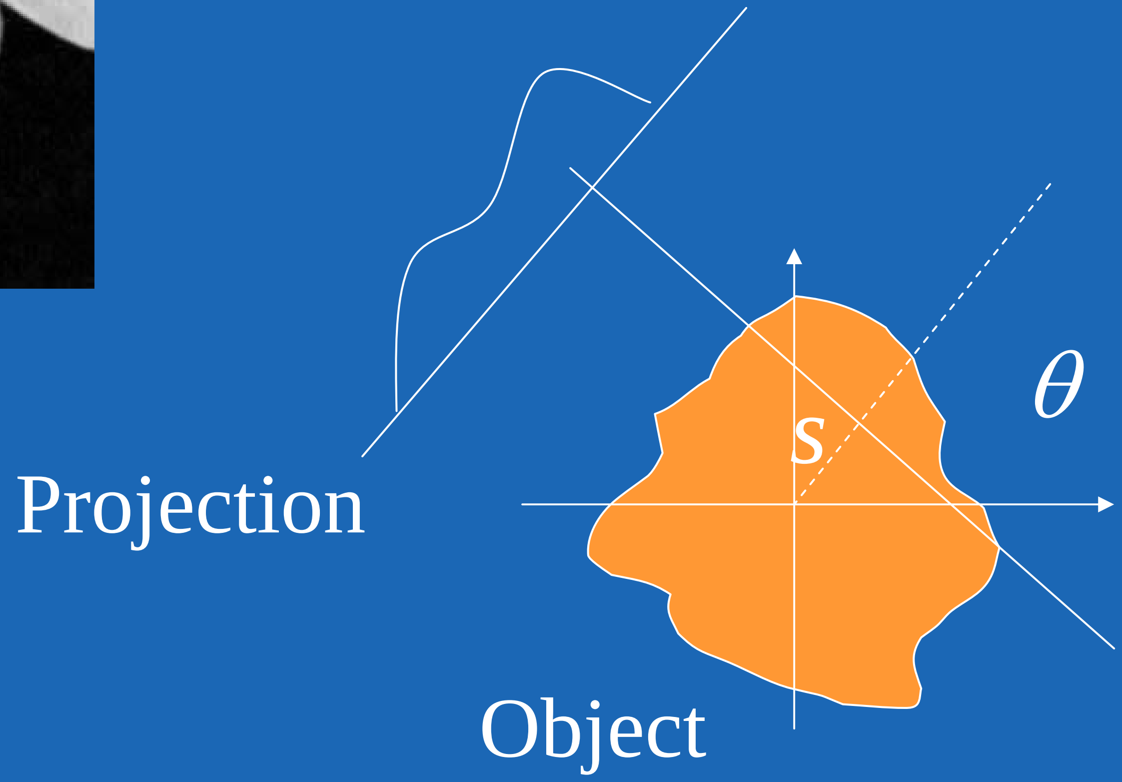

The inverse 3D (Radon) transform
(H.A. Lorentz, 1905)

$$f = \frac{-1}{4\pi^2} \iint \frac{\partial^2}{\partial s^2} \hat{f}(s,\theta,\omega)\, d\theta\, d\omega$$

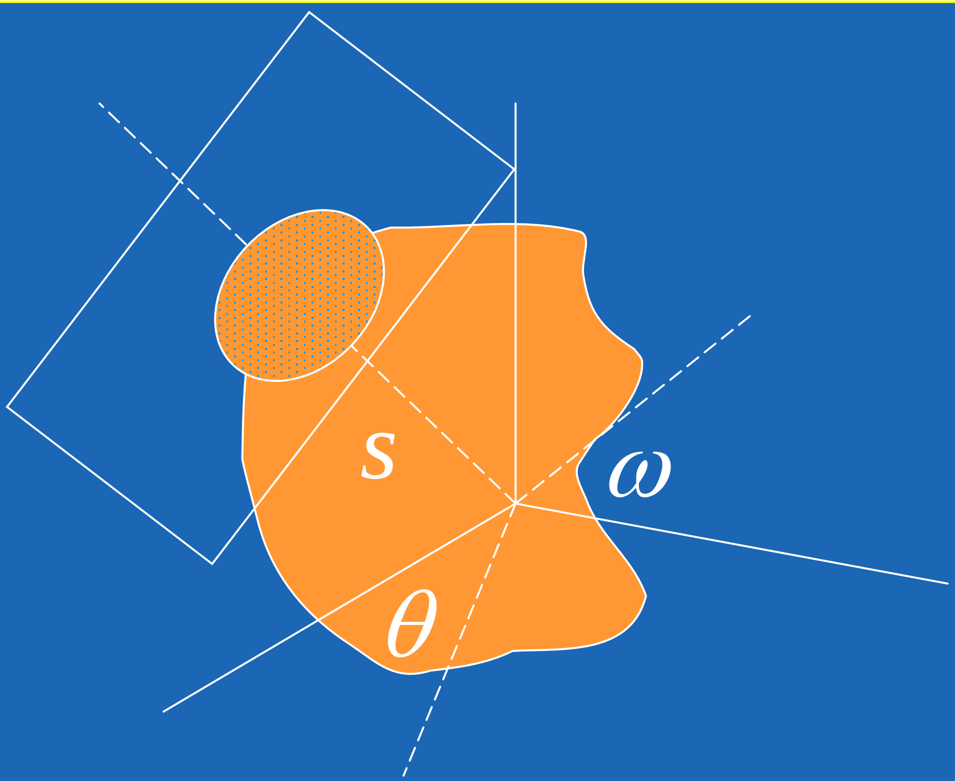

Applications

- Medical imaging
- Laboratory animals

- Materials research
- Non-destructive testing
- Reverse engineering
- Geophysics

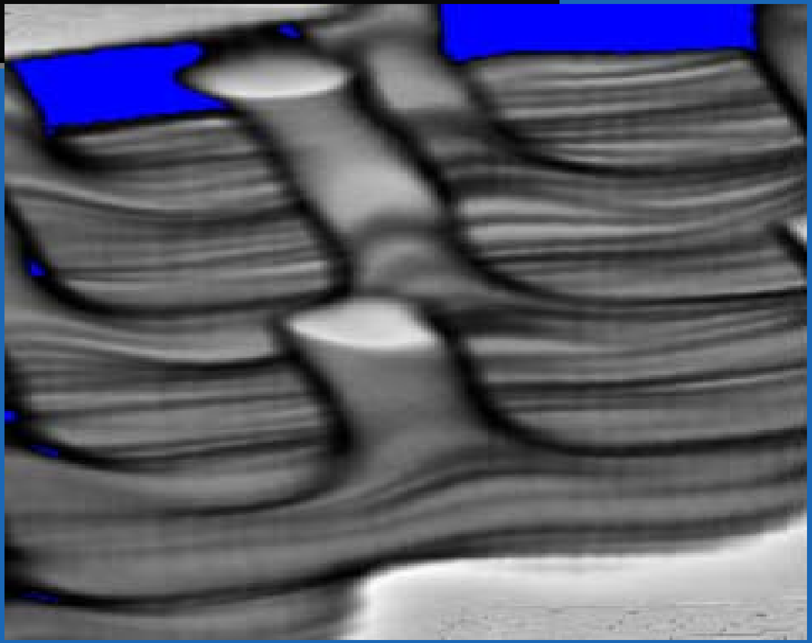

Principle of x-ray tomography

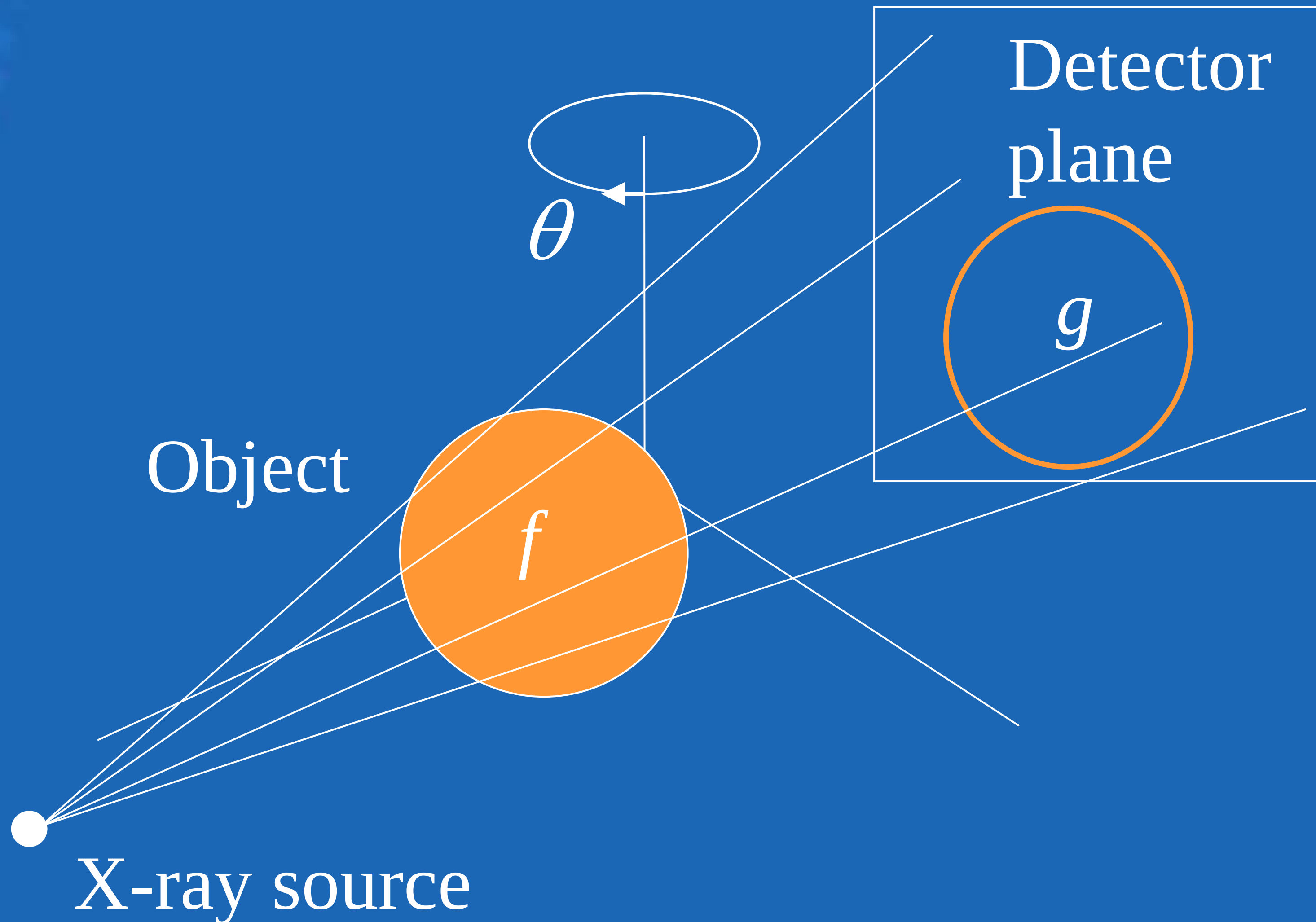

Fourier slice theorem

$$\hat{f}(u_\theta, v_\theta) = \hat{g}_\theta(u, v)$$

Fourier transform in the central plane is the Fourier transform of the projection

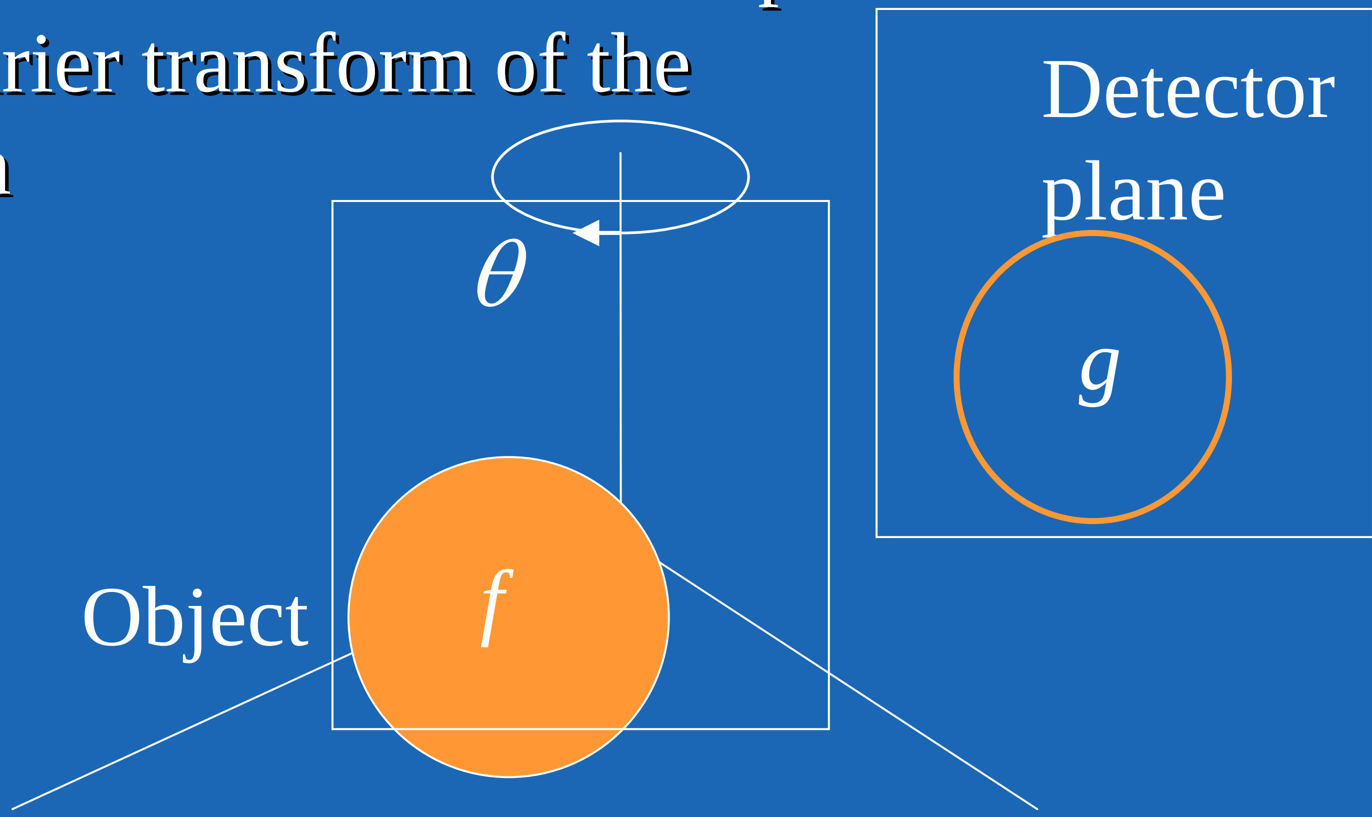

Image reconstruction

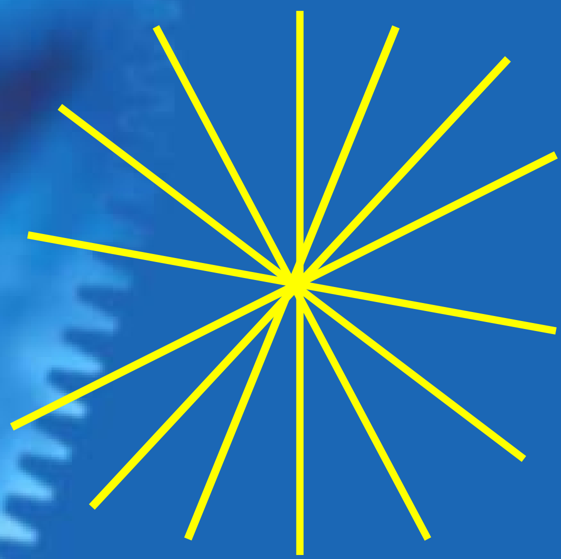

- Filling up the Fourier space

- Filtered backprojection:

$$f = \int_0^{\pi} q * g_\theta \, d\theta$$

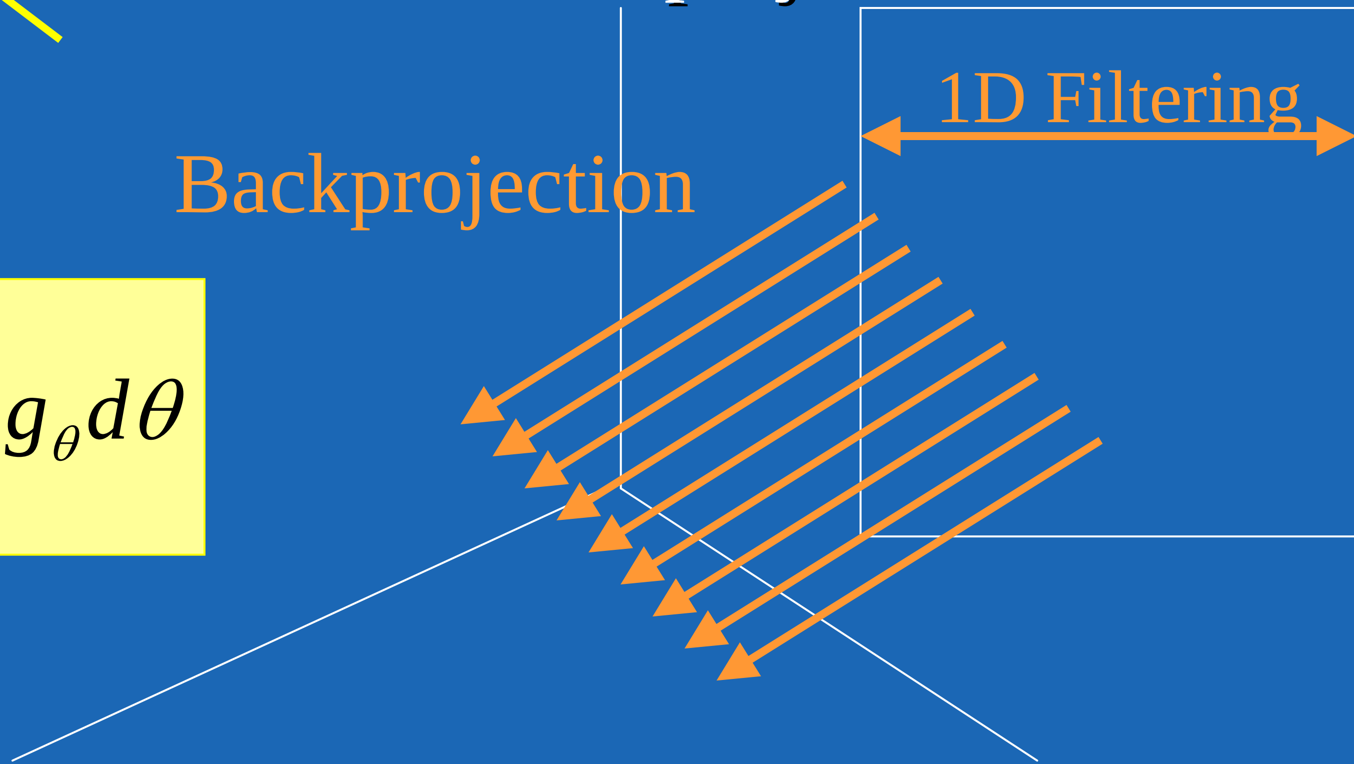

Density reconstruction; non-planar orbits
(Bronnikov, 1995-2002)

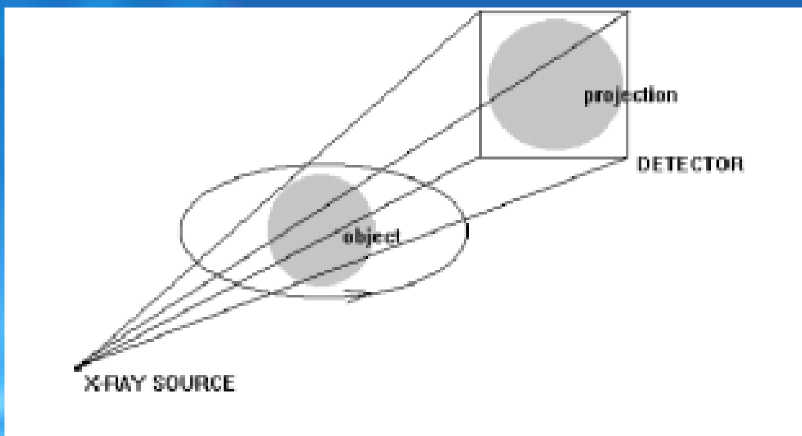

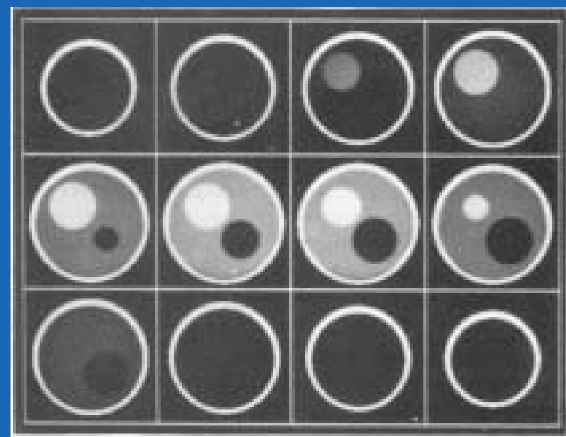

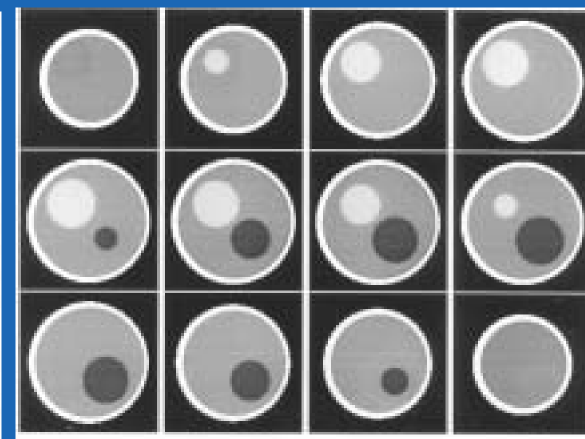

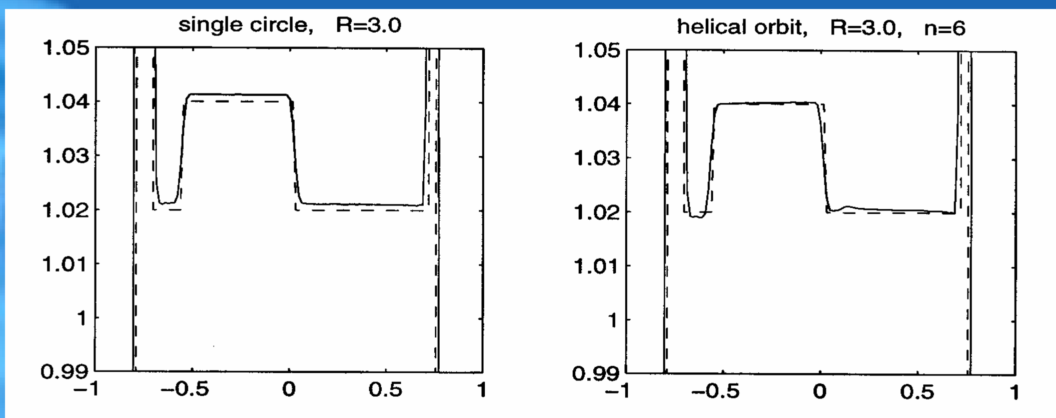

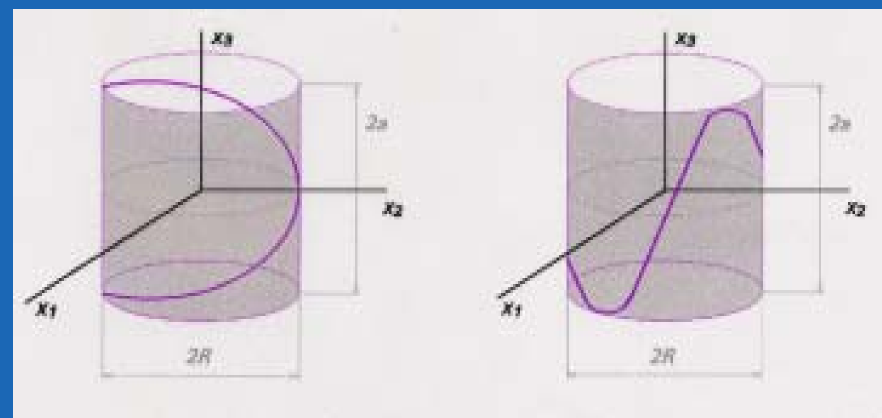

Wavelet-based contrast enhancement

Original image

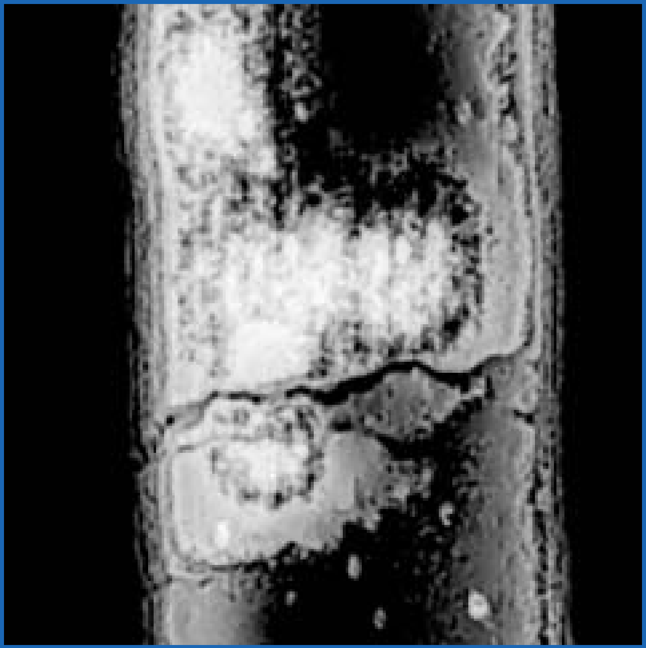

Processed image

Bronnikov and Duifhuis, 1998

Contrast-enhanced imaging

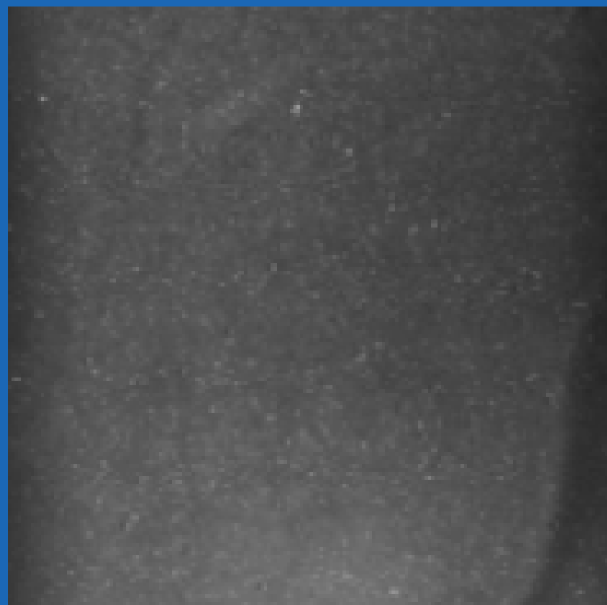

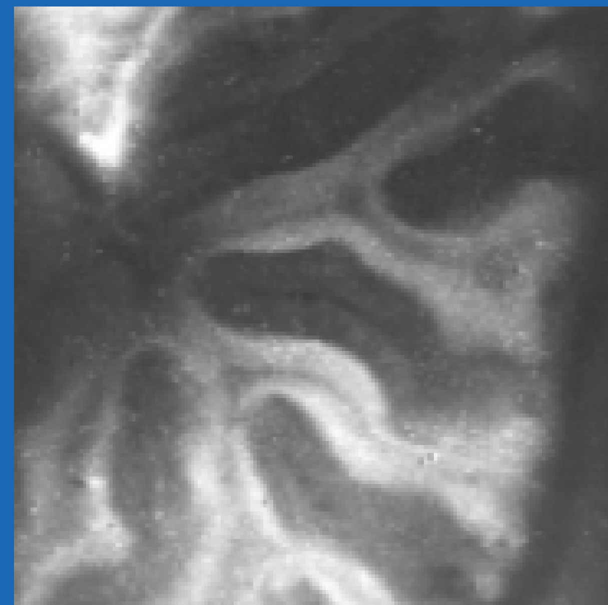

X-ray images of the rat cerebellum

Absorption contrast **Phase contrast**

A. Momose, T. Takeda, Y. Itai and K. Hirao, *Nature Medicine, 2, 473-475 (1996).*

Phase-contrast imaging

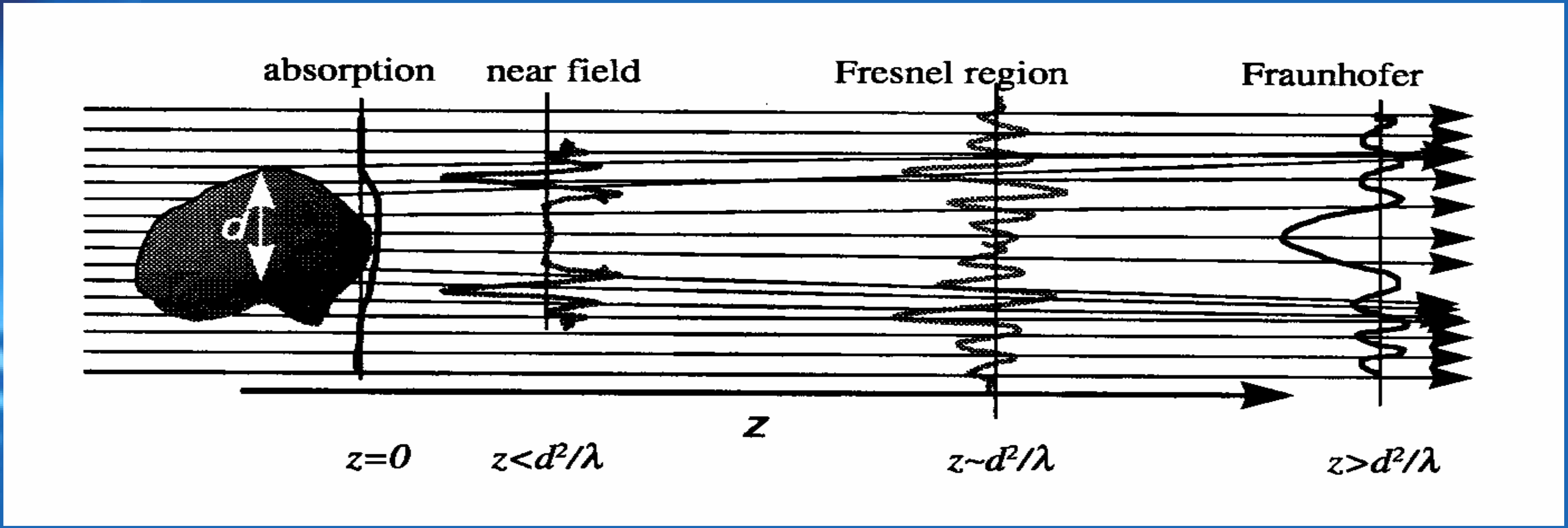

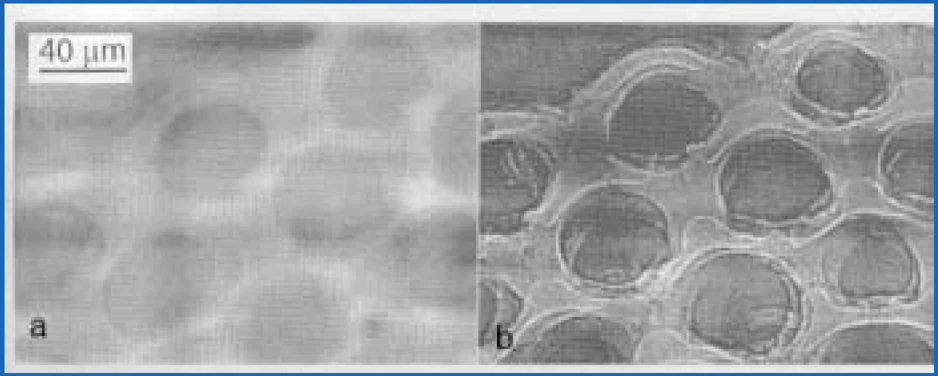

- Coherent x-rays
- Microfocus tube

Phase-contrast CT vs. absorption-contrast CT
(ESRF)

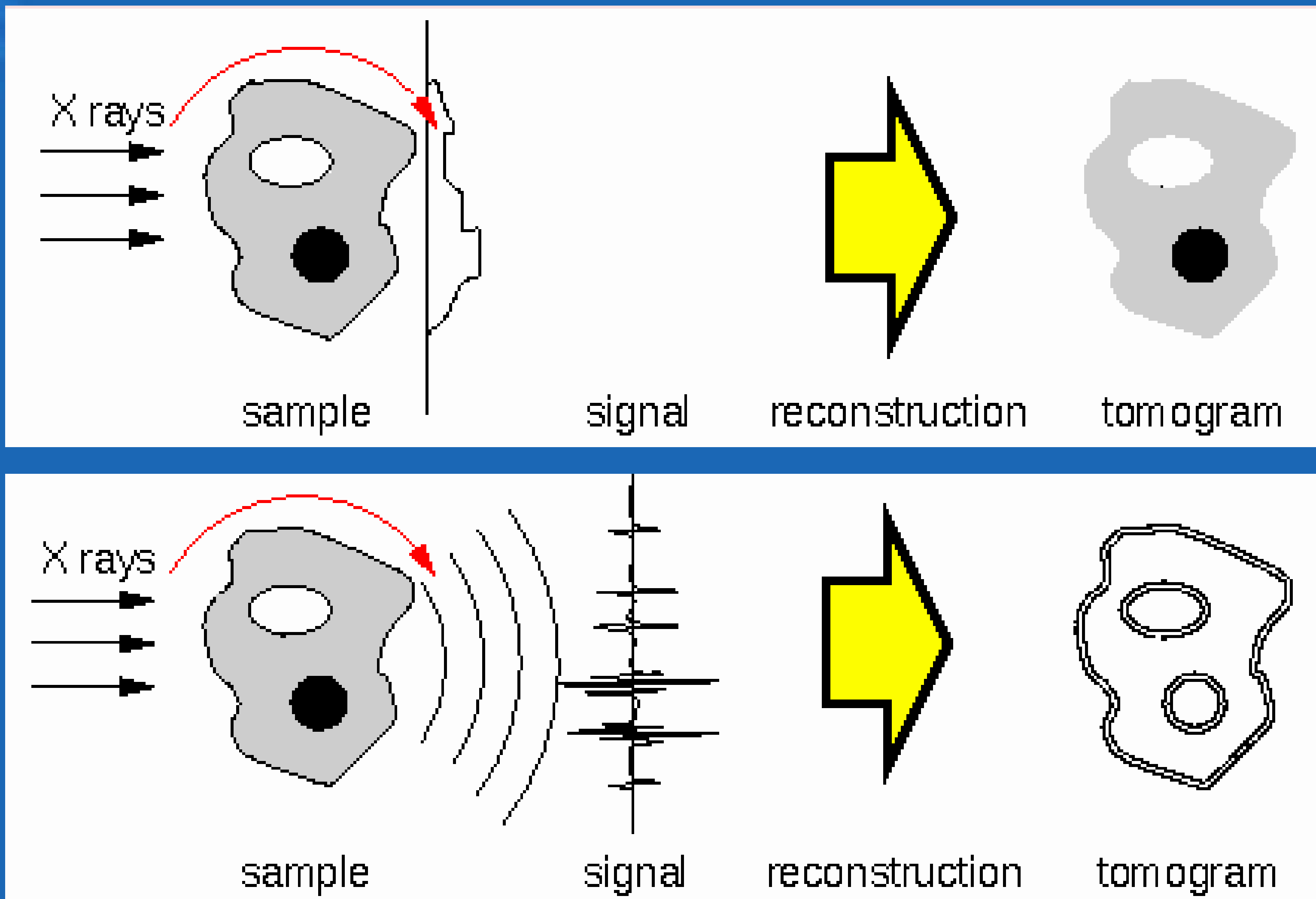

Insect knee E=18 KeV

Snigirev et al, ESRF

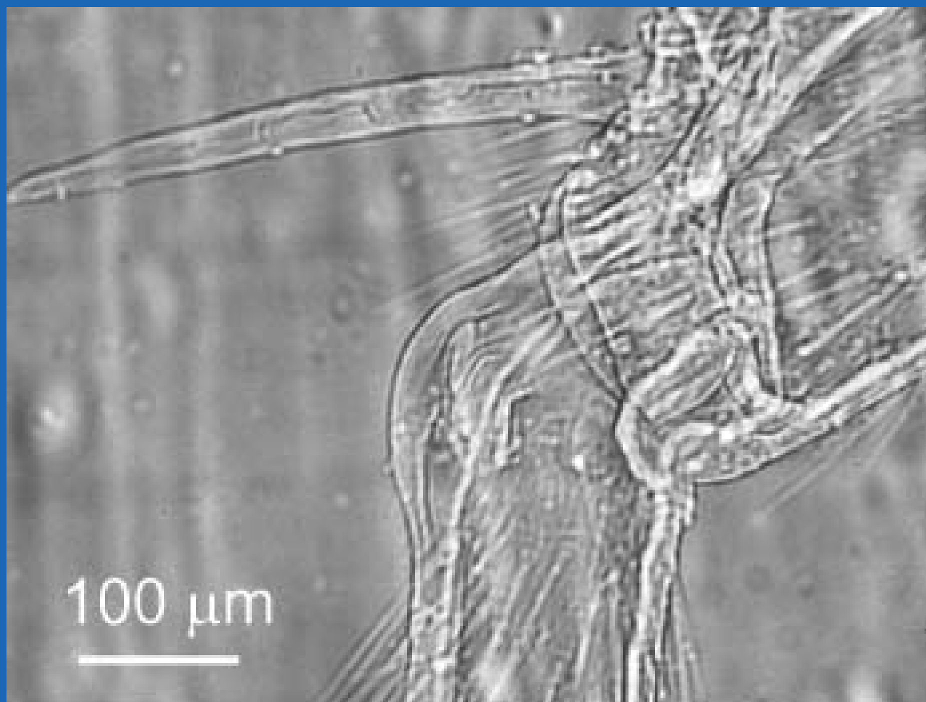

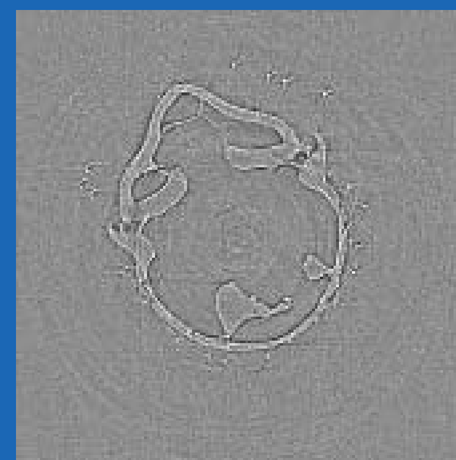

Problems

- the lack of the linear theory comparable to that of conventional absorption-based CT
- no quantitative solution (only edges of the objects are reconstructed)
- huge amount of high-resolution data

Goals

- to develop an accurate and practical mathematical tool for quantitative phase-contrast image reconstruction

- to suggest the fastest image reconstruction algorithm for phase-contrast CT

Inverse problem of phase-contrast tomography

$$\text{find } f(x_1, x_2, x_3) \text{ from } I_\theta^z(x, y), \ 0 \leq \theta < \pi$$

- Phase retrieval (holographic) approach **(Cloetens et al 1999):**

  - find the phase from intensity
  - invert Radon transform to reconstruct the object

- Reconstruction formula (CT approach):

  - a straightforward linear relation between the intensity and the object function

Phase retrieval

- Nonlinear iterative methods (Gershberg, Saxton 1972; Fienup, 1982)
- Linear TIE method (Gureyev et al, 2004)
- Linear Wigner transform (Maier, Preobrazshenski 1990; Raymer et al 1994)

Wigner transform

$$W_z(x,\xi) = \int_{-\infty}^{\infty} \left\langle V_z^*(x - \frac{x'}{2}) V_z(x + \frac{x'}{2}) \right\rangle e^{-2\pi i \xi x'} dx'$$

$$I(x,z) \overset{Radon\ \ transform}{\Rightarrow} W_0(x,\xi) \overset{Inverse\ \ Wigner}{\Rightarrow} V_0^*(x)V_0(0) \Rightarrow \varphi(x)$$

Radon-Wigner transform

$$\int_{-\infty}^{\infty}\int_{-\infty}^{\infty} W_0(x',\xi)\,\delta(x - z\xi - x')\,dx'\,d\xi = I(x,z)$$

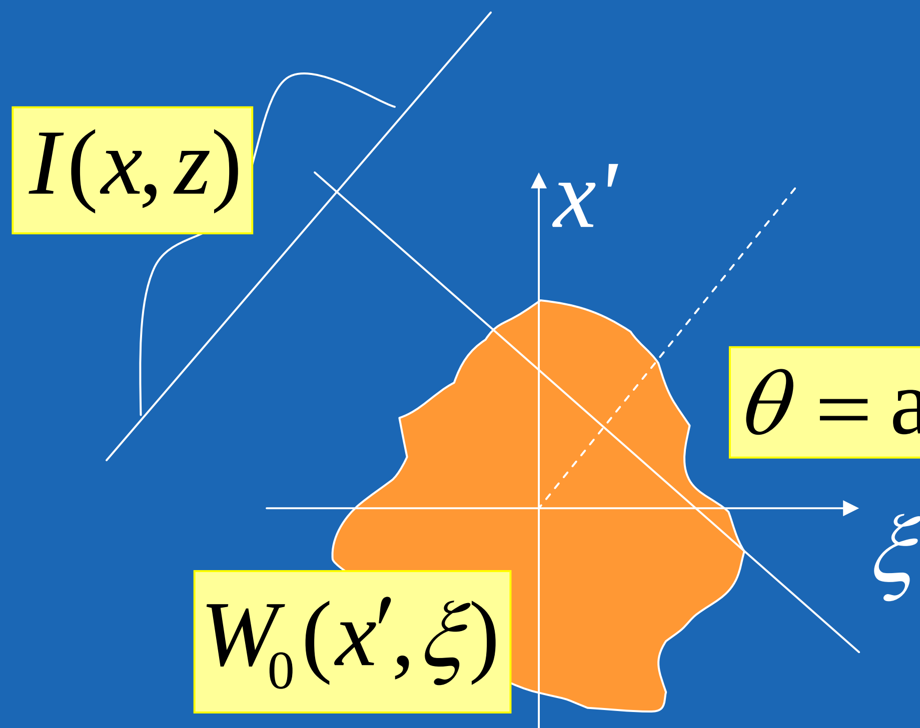

Implementation (Bronnikov et al 1991)

n - number of samples of the discrete Wigner function

$$\text{Number of detection planes} \geq \frac{\pi n}{2}$$

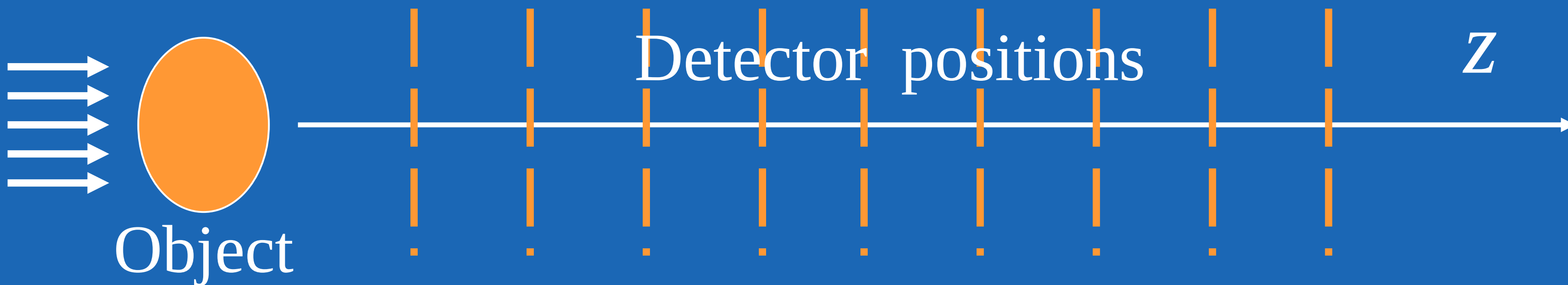

$$I(x,z) \overset{Radon\ transform}{\Rightarrow} W_0(x,\xi) \overset{Inverse\ Wigner}{\Rightarrow} V_0^{\,*}(x)V_0(0) \Rightarrow \varphi(x)$$

Inverse problem of phase-contrast tomography

$$\text{find } f(x_1, x_2, x_3) \text{ from } I_\theta^z(x, y),\ 0 \le \theta < \pi$$

- Phase retrieval (holographic) approach:
  - find the phase from intensity
  - invert Radon transform to reconstruct the object
  - multiple detector positions along the beam

- Reconstruction formula (CT approach):
  - a straightforward linear relation between the intensity and the object function
  - single detector position

Mathematical model: the Fresnel propagator

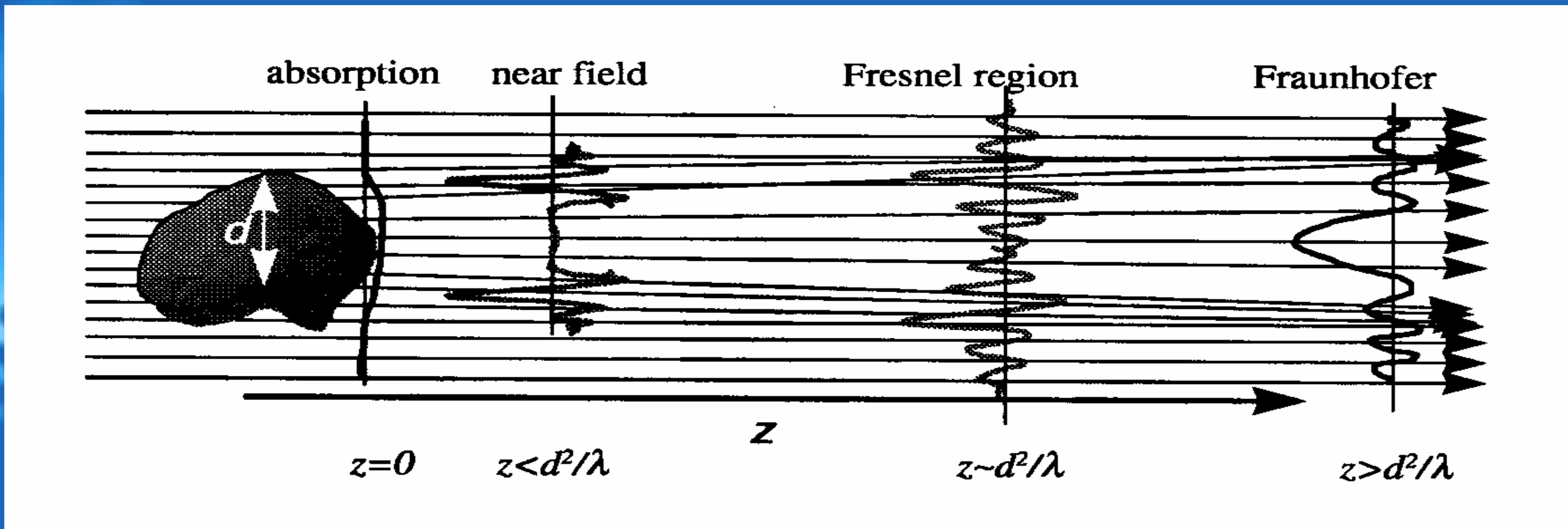

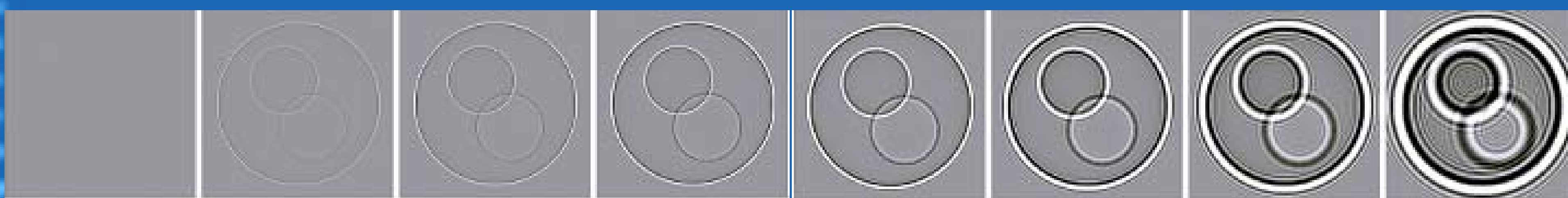

Theoretical background

$$T_\theta(x,y) = e^{-\frac{1}{2}\mu_\theta(x,y)+i\varphi_\theta(x,y)}$$

Transmission function

$$U_\theta(x,y) = T_\theta(x,y)\,U_i$$

Wavefield

$$I_\theta^z(x,y) = \left| h_z ** U_\theta \right|^2, \quad 0 \le \theta < \pi$$

Fresnel propagation

$$\lambda d < D^2 \qquad \left|\frac{\partial \mu_\theta}{\partial x}\right|, \left|\frac{\partial \mu_\theta}{\partial y}\right| \to 0$$

Conditions

$$I_\theta^d(x,y) = I_\theta^0 \left[1 - \frac{\lambda d}{2\pi} \nabla^2 \varphi_\theta(x,y) \right]$$

Intensity equation

Radon transforms

2D transform (lines)

$$\hat{f}_{\omega,s} = \int_{Line\ (\omega,s)} f\ dl$$

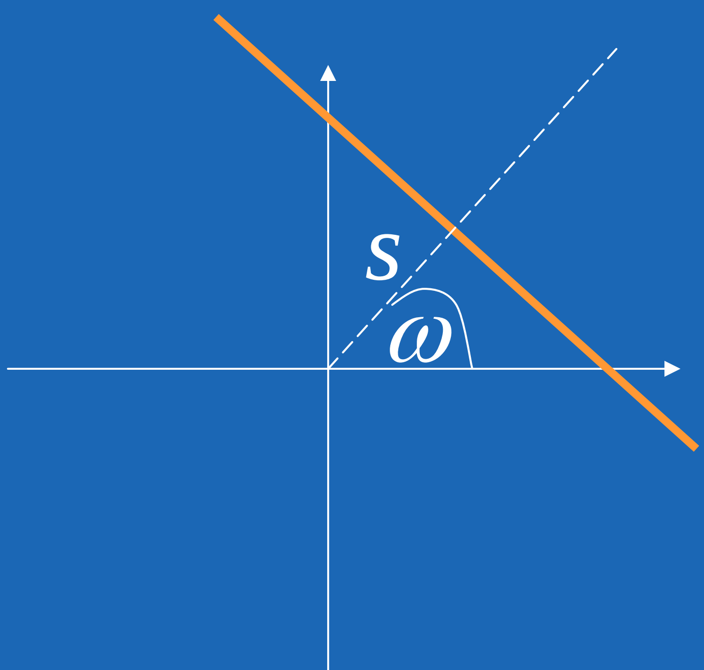

3D transform (planes)

$$\hat{f}_{\theta,\omega,s} = \int_{Plane\ (\theta,\omega,s)} f\ d\sigma$$

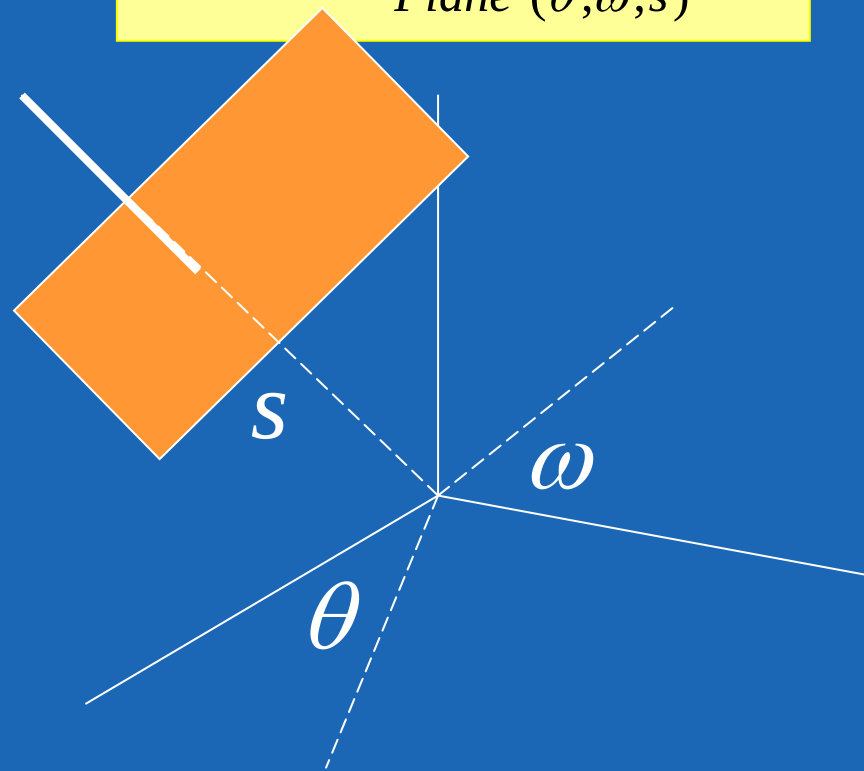

Fundamental theorem (Bronnikov 2002)

Second derivative of 3D Radon transform of the object is proportional to 2D Radon transform of the phase-contrast projection

$$\frac{\partial^2}{\partial s^2}\hat{f}(s,\theta,\omega) = \frac{-1}{d}\hat{g}_\theta(s,\omega)$$

$$\lambda d < D^2$$

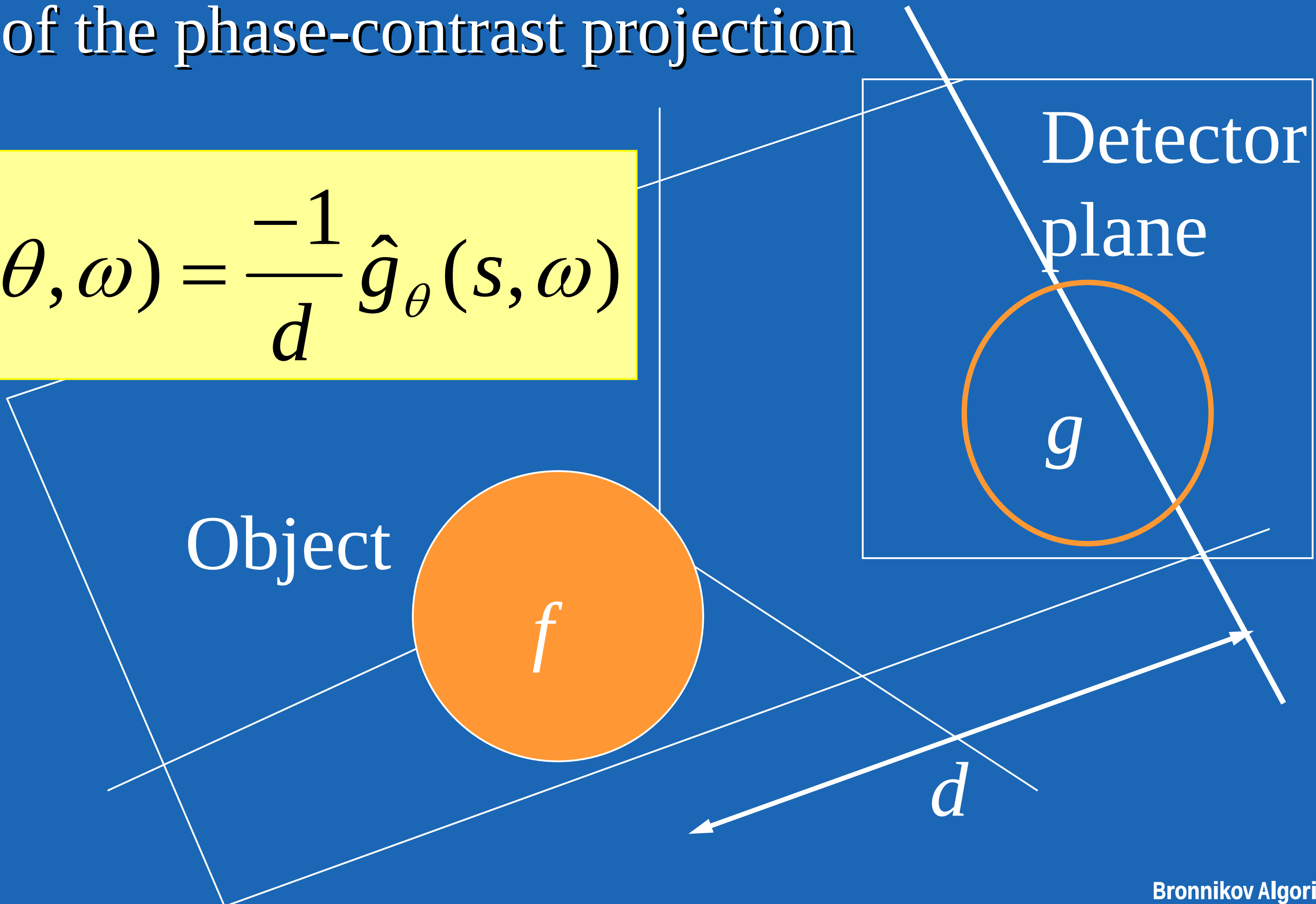

Inversion formula (Bronnikov 1999)

$$f = \frac{-1}{4\pi^2}\iint \frac{\partial^2}{\partial s^2}\hat{f}(s,\theta,\omega)\,d\theta\, d\omega = \frac{1}{4\pi^2 d}\iint \hat{g}_\theta(s,\omega)\,d\theta\, d\omega$$

3D backprojection of the 2D Radon transform of the phase-contrast projection

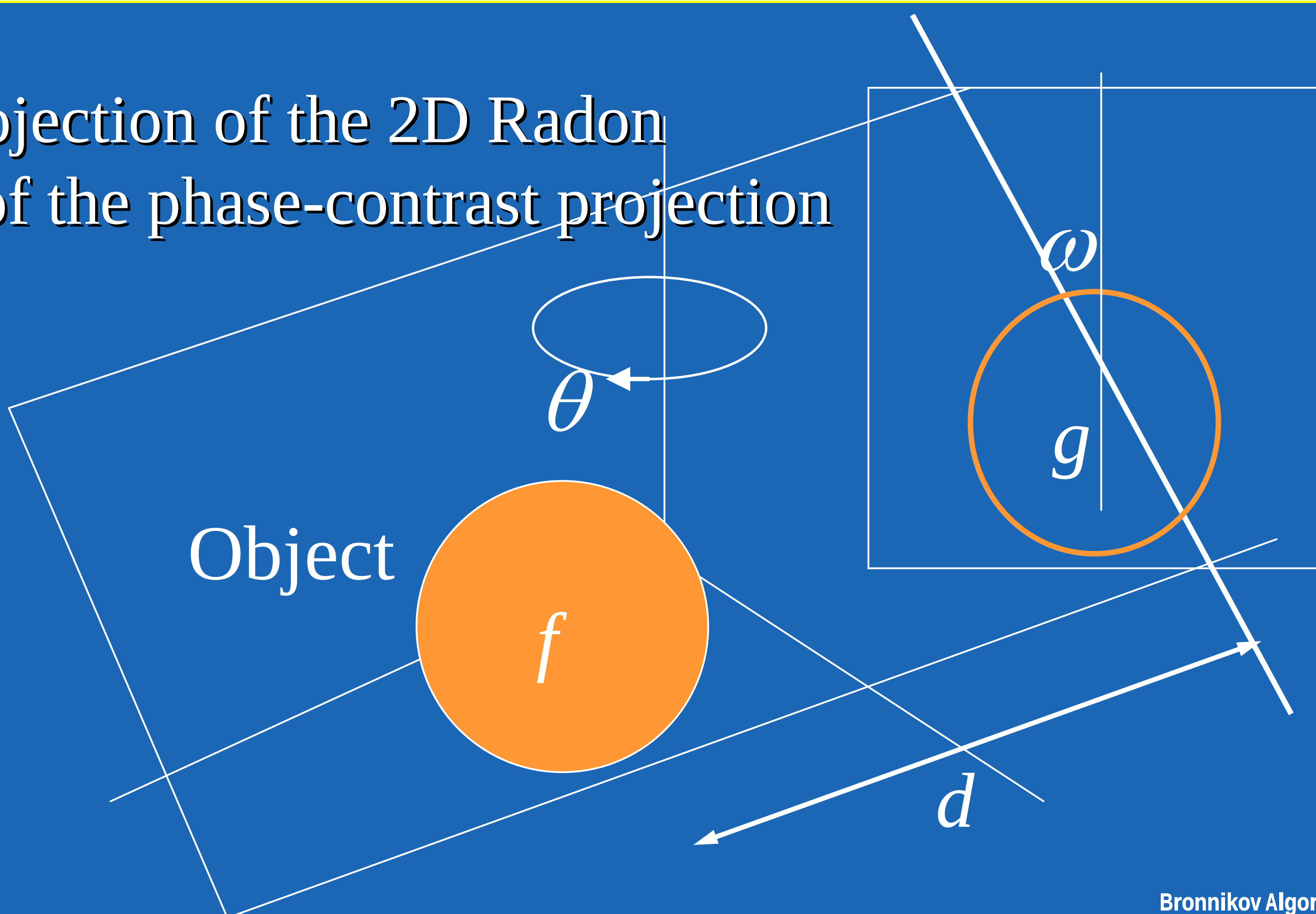

FBP algorithm (Bronnikov 1999, 2002)

$$f = \frac{1}{4\pi^2 d}\int_0^{\pi} q ** g_\theta \, d\theta$$

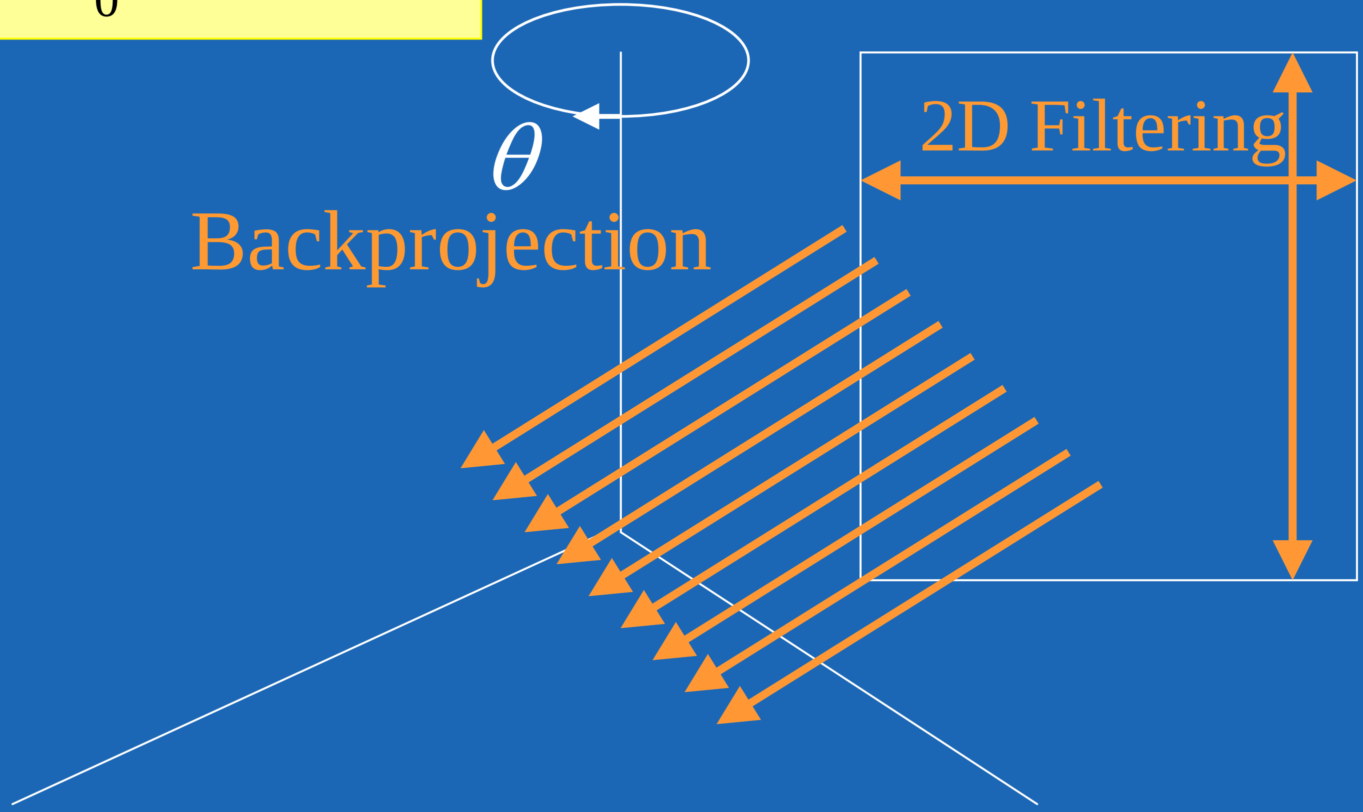

Analytical filter function (Bronnikov 1999, 2002)

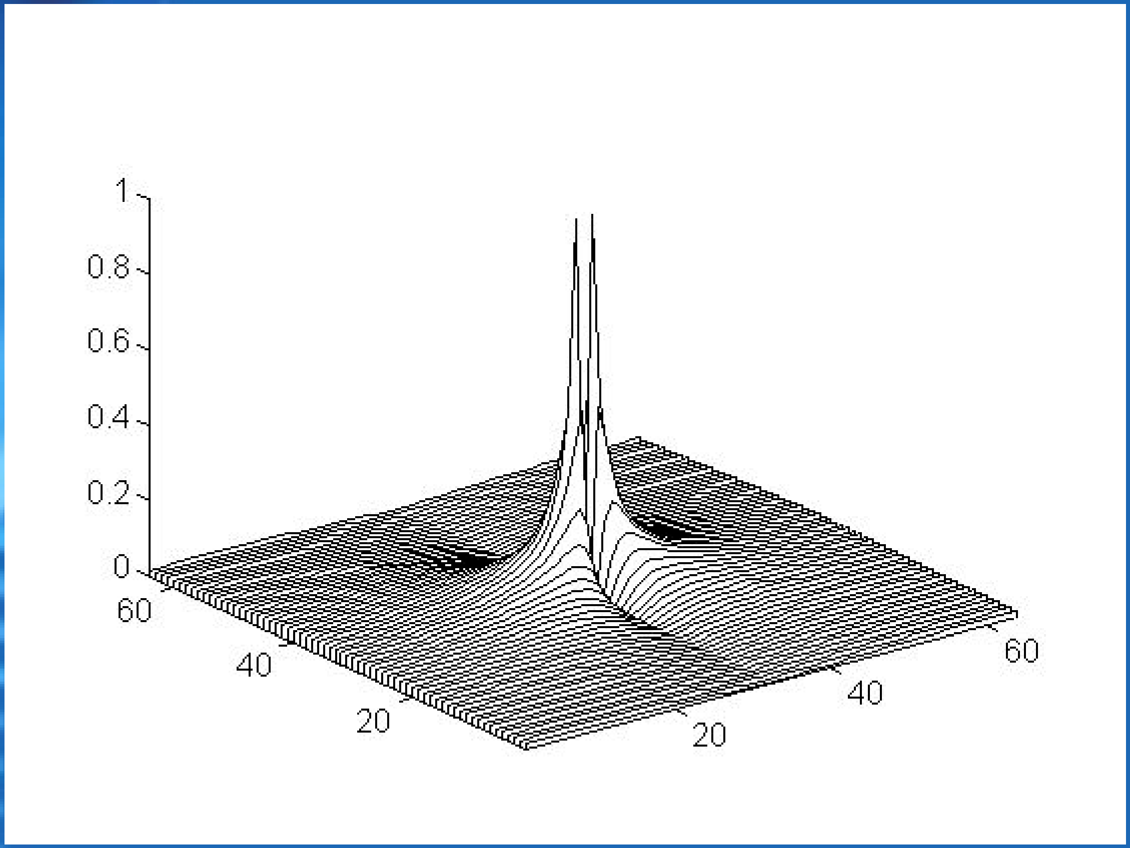

$$f = \frac{1}{4\pi^2 d}\int_0^{\pi} q ** g_\theta \, d\theta$$

$$q = \frac{|y|}{x^2 + y^2}$$

MTF of the 2D filter:

$$Q = \frac{|\xi|}{\xi^2 + \eta^2}$$

Implementation

- FFT-based linear filtering
- 2D parallel-beam backpojection
- FBP structure (parallelization)
- Hardware acceleration

→ The fastest algorithm possible

Phase object

$$g_\theta(x,y) = I_\theta^d / I_i - 1$$

$$f = \frac{1}{4\pi^2 d} \int_0^\pi q ** g_\theta \, d\theta$$

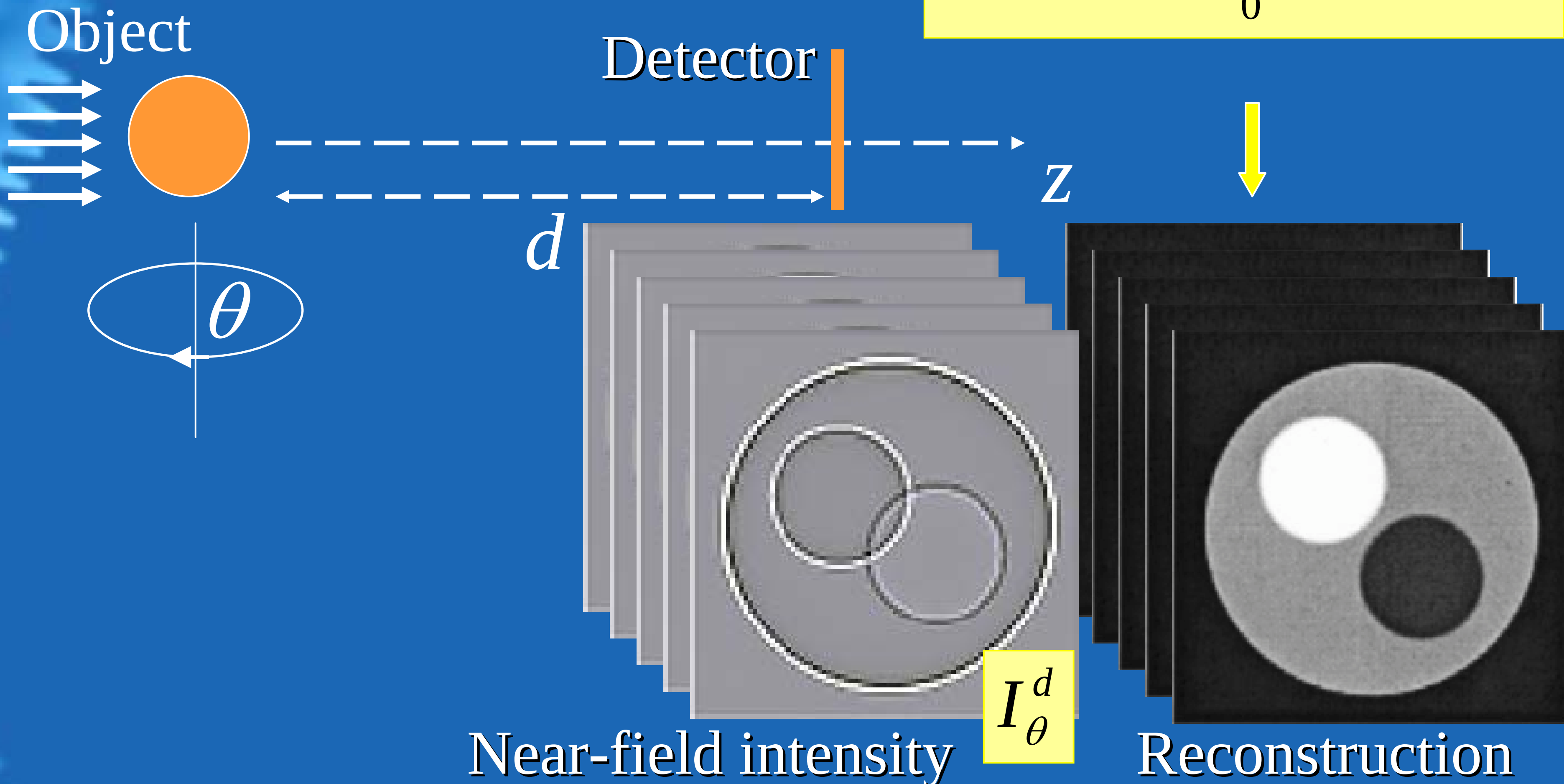

Phantom studies: polystyrene sphere

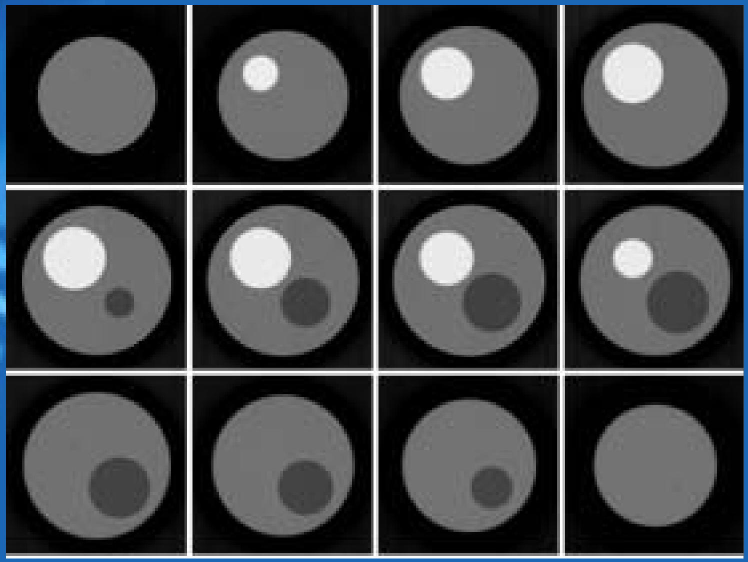

3D computer phantom

d = 2.5 cm

λ = 0.1 nm, Δ = 1 μm

3D reconstruction

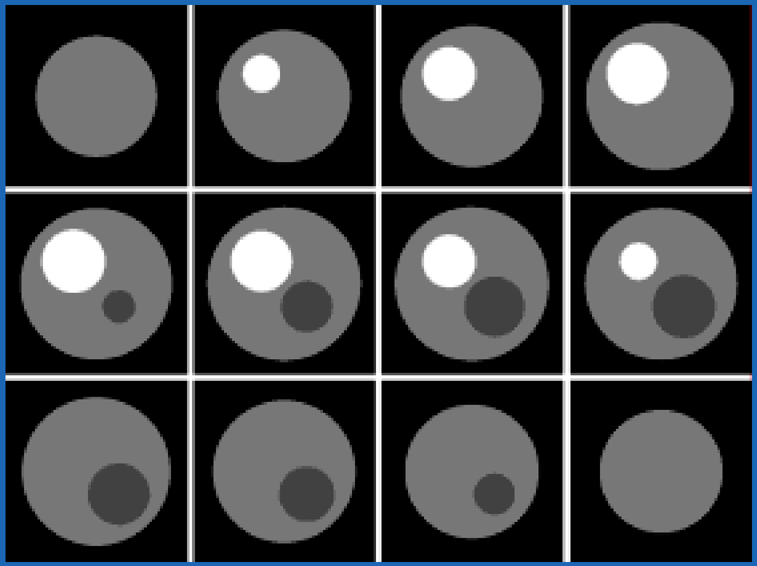

Phase-contrast projections

Quantification and the limits of the linear approximation

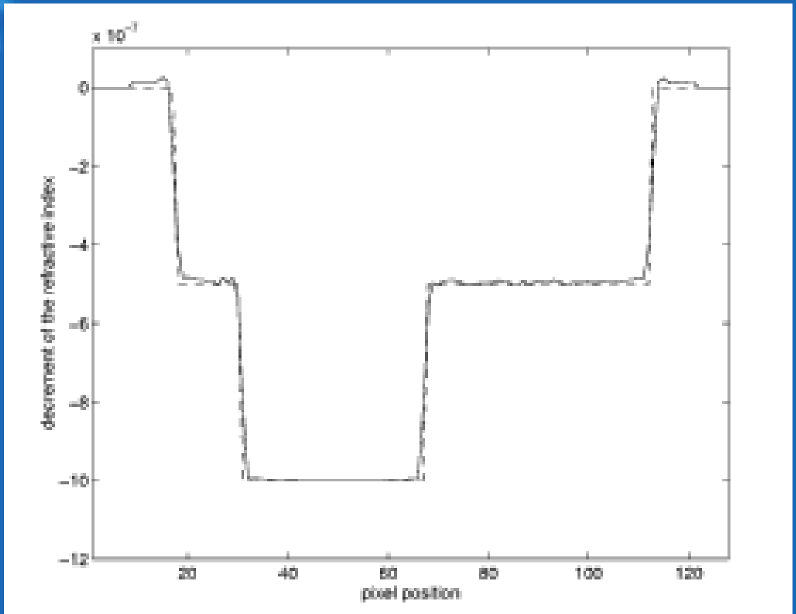

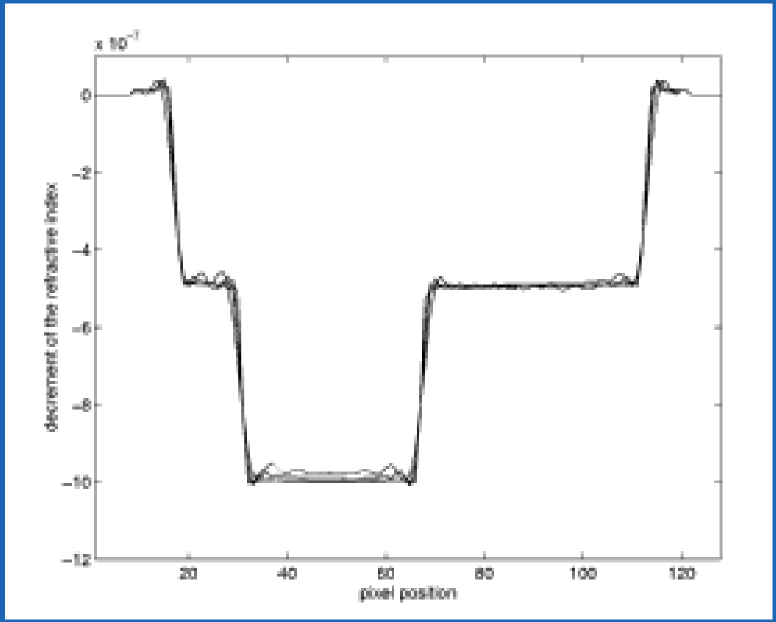

$d = 2.5$ cm

$1.5 < d < 20$ cm

Stability to noise

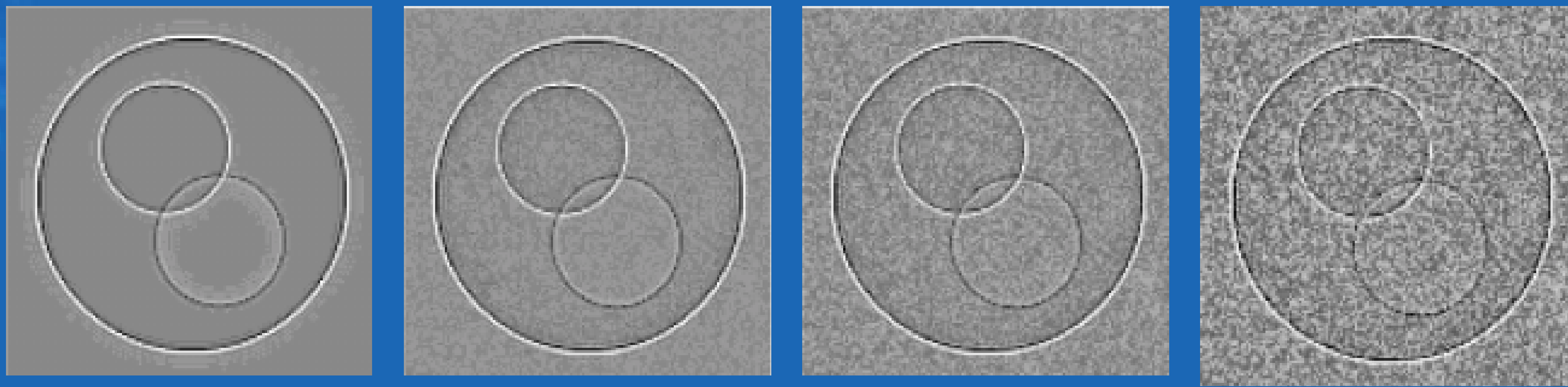

0% 1% 2% 5%

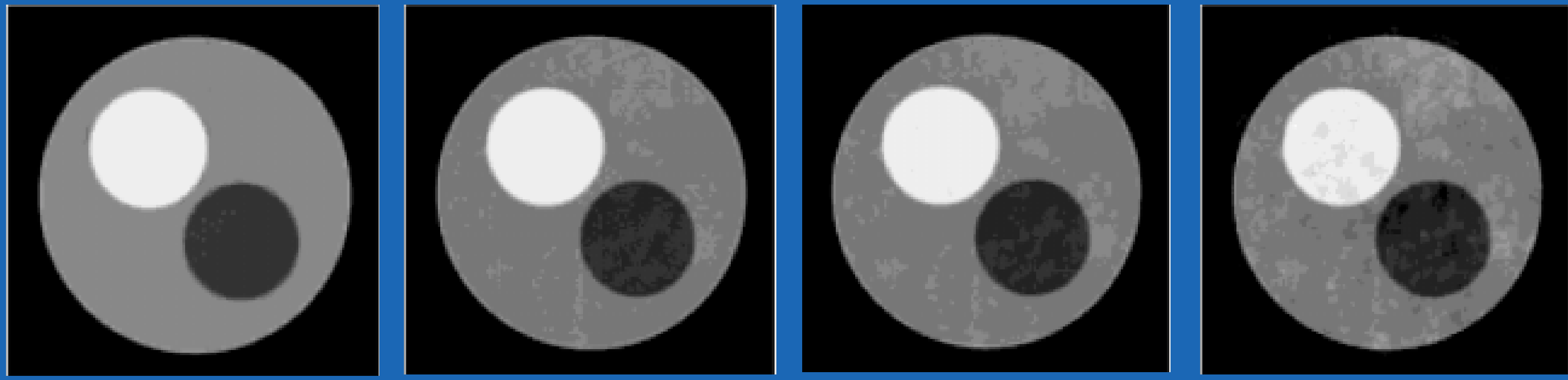

Mixed phase and amplitude object

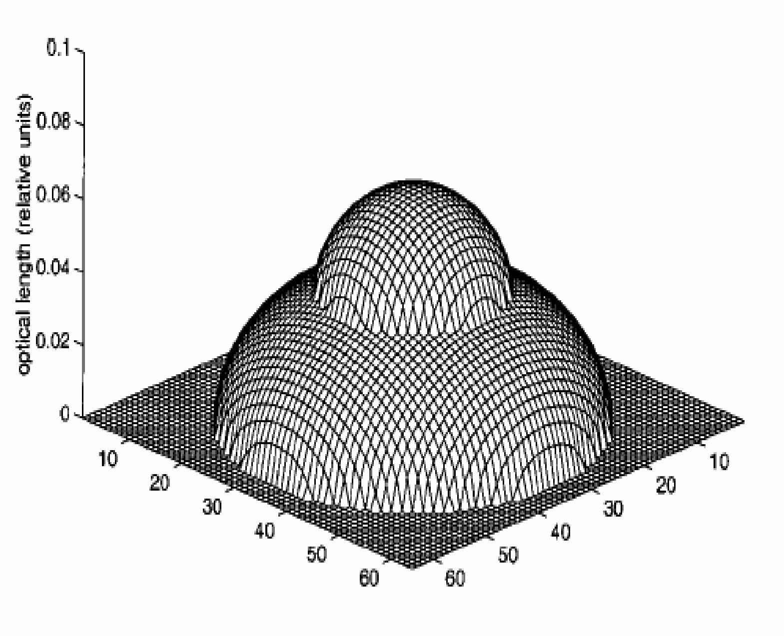

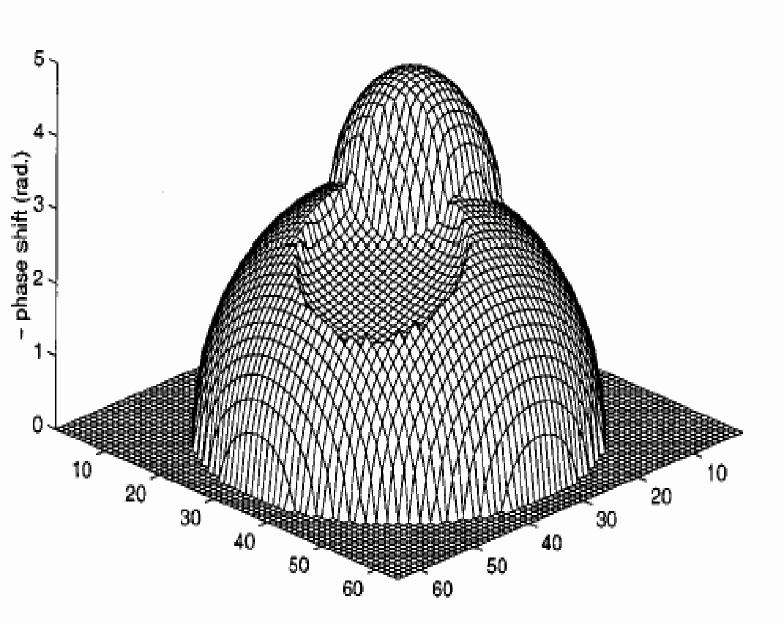

Absorption function μ/2 Phase function φ

$$T(x,y) = e^{-\frac{1}{2}\mu(x,y)+i\varphi(x,y)}$$

Mixed phase and amplitude object

$$g_\theta(x,y) = I_\theta^d / I_\theta^0 - 1$$

$$f = \frac{1}{4\pi^2 d}\int_0^\pi q ** g_\theta \, d\theta$$

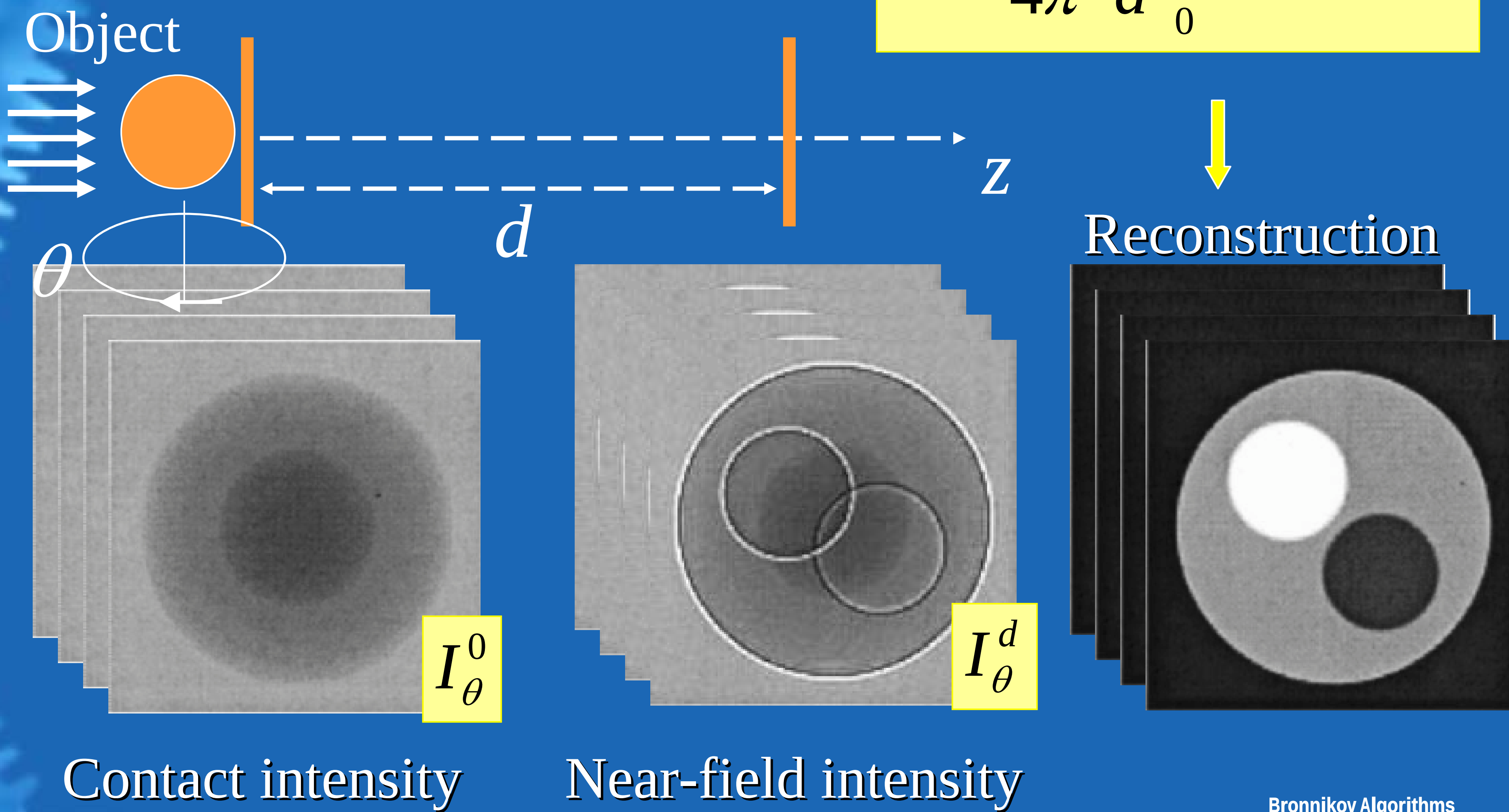

Bronnikov Algorithms

Comparison with heuristic methods

(Anastasio et al, PMB 2003)

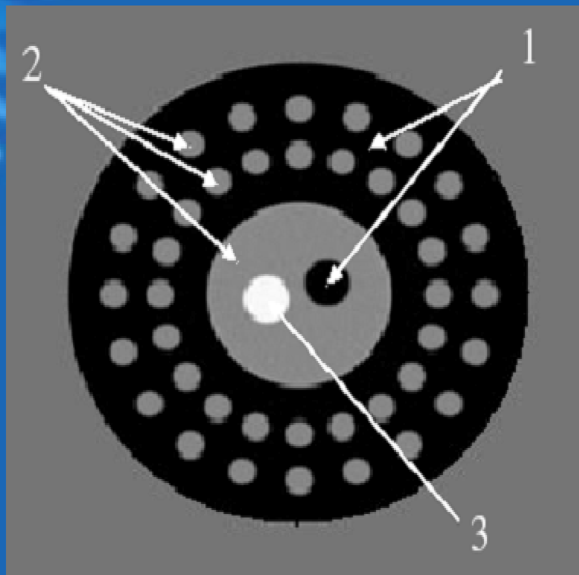

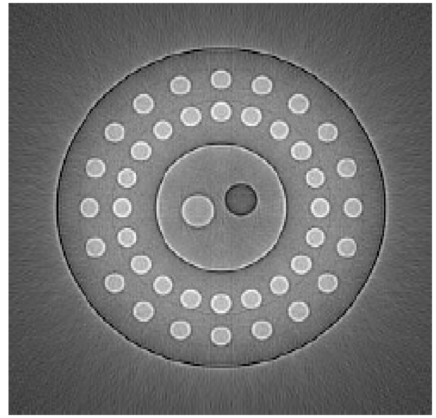

Backprojection

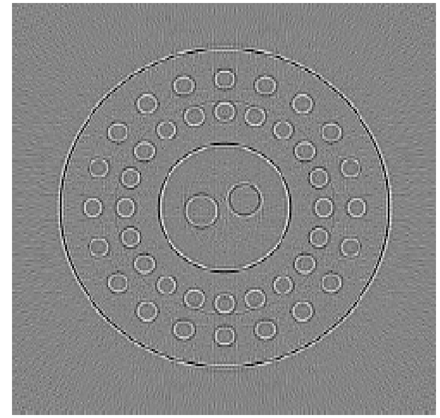

“Absorption” FBP

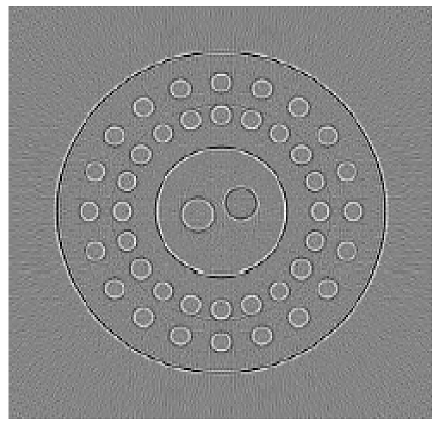

“Absorption” LFBP

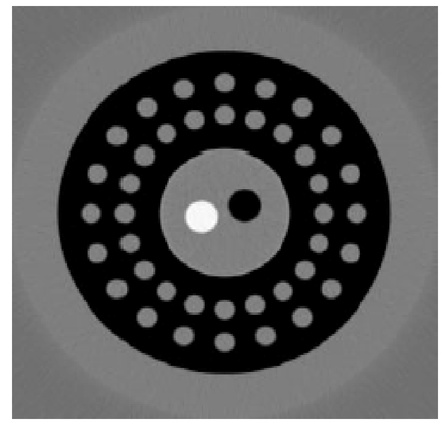

Bronnikov method

Polypropylene foam

(Schena et al; Elettra, 2004)

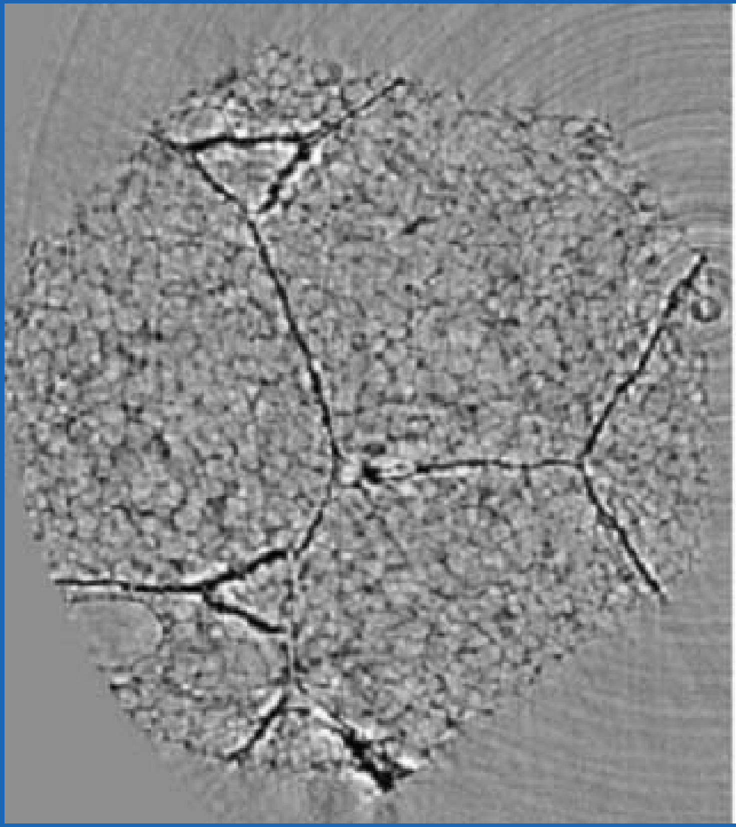

Conventional FPB

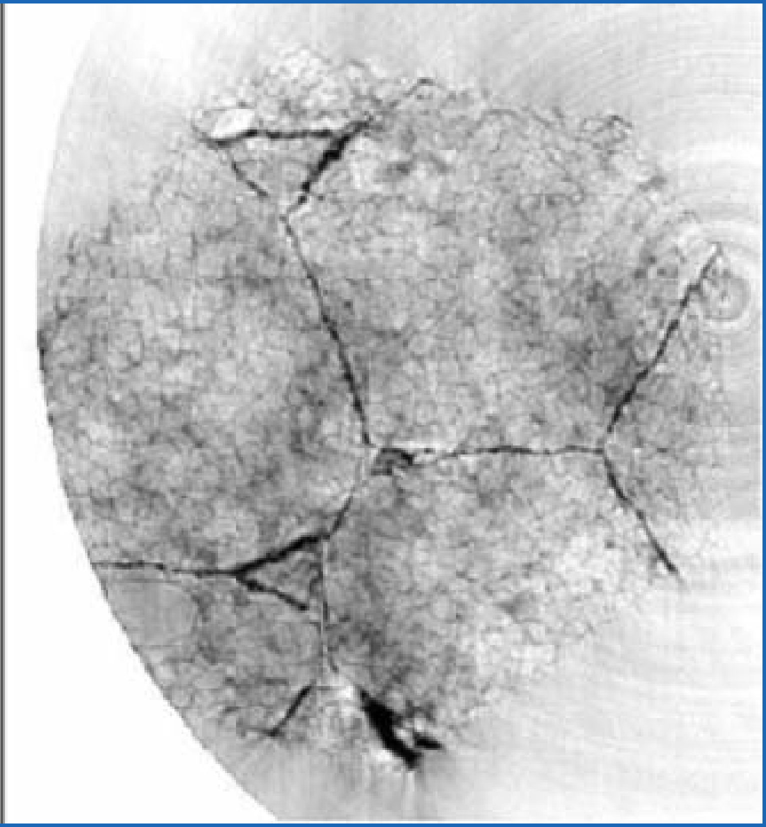

Bronnikov method

Polyethylene tube with polymer fibers
(Groso and Stampanoni; SLS, 2005)

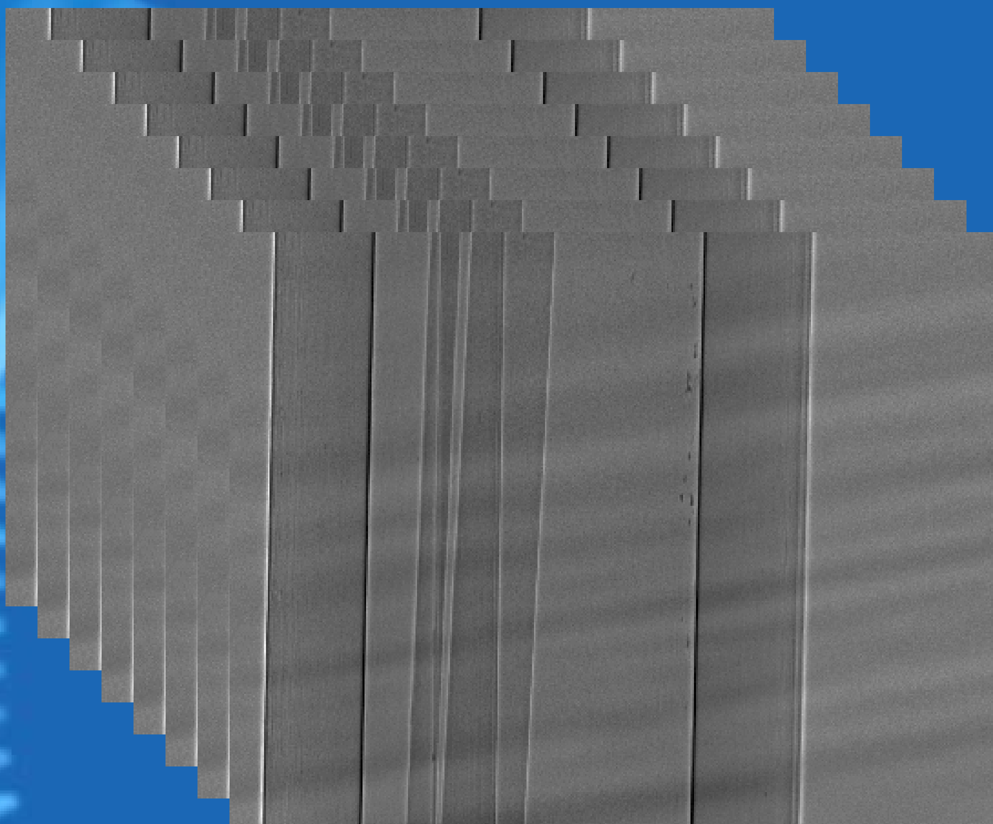

721 projections; 15 cm distance sample detector; Energy=13.5 keV
Pixel size 1.75 microns

Summary

- A fundamental theorem has been proved. This is the counterpart of the Fourier slice theorem used in absorption-based CT
- A fast image reconstruction algorithm has been implemented in the form of filtered backprojection (FBP)